NeuroImage: Clinical 42 (2024) 103617

Contents lists available at ScienceDirect

NeuroImage: Clinical

journal homepage: www.elsevier.com/locate/ynicl

Structural and microstructural predictors of cognitive decline in deep brain stimulation of subthalamic nucleus in Parkinson's disease

Pavel Filip [a,b,c], Josef Mana [a], Andrej Lasica [a], Jiří Keller [d,e], Dušan Urgošík [f], Jaromír May [f], Karsten Mueller [a,g], Robert Jech [a,*,1], Ondrej Bezdicek [a,1], Filip Růžička [a,1]

[a] Department of Neurology, Charles University, First Faculty of Medicine and General University Hospital, Prague, Czech Republic
[b] Department of Cybernetics, Czech Technical University in Prague, Prague, Czech Republic
[c] Center for Magnetic Resonance Research (CMRR), University of Minnesota, Minneapolis, MN, USA
[d] Department of Radiology, Na Homolce Hospital, Prague, Czech Republic
[e] Third Faculty of Medicine, Charles University in Prague, Prague, Czech Republic
[f] Department of Stereotactic and Radiation Neurosurgery, Na Homolce Hospital, Prague, Czech Republic
[g] Max Planck Institute for Human Cognitive and Brain Sciences, Leipzig, Germany

ARTICLE INFO

Keywords:
Deep brain stimulation
Parkinson's disease
Subthalamic nucleus
Diffusion weighted imaging
Diffusion tensor imaging

ABSTRACT

Background and objectives: The intricate relationship between deep brain stimulation (DBS) in Parkinson's disease (PD) and cognitive impairment has lately garnered substantial attention. The presented study evaluated pre-DBS structural and microstructural cerebral patterns as possible predictors of future cognitive decline in PD DBS patients.

Methods: Pre-DBS MRI data in 72 PD patients were combined with neuropsychological examinations and follow-up for an average of 2.3 years after DBS implantation procedure using a screening cognitive test validated for diagnosis of mild cognitive impairment in PD in a Czech population – Dementia Rating Scale 2.

Results: PD patients who would exhibit post-DBS cognitive decline were found to have, already at the pre-DBS stage, significantly lower cortical thickness and lower microstructural complexity than cognitively stable PD patients. Differences in the regions directly related to cognition as bilateral parietal, insular and cingulate cortices, but also occipital and sensorimotor cortex were detected. Furthermore, hippocampi, putamina, cerebellum and upper brainstem were implicated as well, all despite the absence of pre-DBS differences in cognitive performance and in the position of DBS leads or stimulation parameters between the two groups.

Conclusions: Our findings indicate that the cognitive decline in the presented PD cohort was not attributable primarily to DBS of the subthalamic nucleus but was associated with a clinically silent structural and microstructural predisposition to future cognitive deterioration present already before the DBS system implantation.

1. Introduction

The concept of Parkinson's disease (PD) has gradually developed from that of a motor disorder to a multi-faceted brain disease affecting virtually all domains, including cognition. Indeed, more than a third of PD patients exhibit signs of cognitive decline, ranging from mild cognitive impairment (MCI) to overt dementia (Cammisuli et al., 2019). Not only is the effect of cognitive impairment on the quality of life often devastating, but it may also be considered a partial contraindication to more complex therapeutic modalities as deep brain stimulation (DBS) of the subthalamic nucleus (STN). Lower baseline cognitive performance has been previously associated with worse outcomes of STN DBS

Abbreviations: MRI, magnetic resonance imaging; T1w, T1-weighted; DBS, deep brain stimulation; STN, subthalamic nucleus; PD, Parkinson's disease; YOPD, young-onset Parkinson's disease; VTA, Volume of Tissue Activated; ROI, Region of Interest; MNI, Montreal Neurological Institute; CIFTI, Connectivity Informatics Technology Initiative; HCP, Human Connectome Project; FDR, False Discovery Rate; DWI, diffusion weighted imaging; DTI, diffusion tensor imaging; DRS-2, Dementia Rating Scale.

* Corresponding author at: Department of Neurology, First Faculty of Medicine, Charles University and General University, Hospital in Prague, Kateřinská 30, 120 00 Prague, Czech Republic.
E-mail address: jech@cesnet.cz (R. Jech).
[1] Authors contributed equally to the study.

https://doi.org/10.1016/j.nicl.2024.103617
Received 16 January 2024; Received in revised form 22 March 2024; Accepted 6 May 2024
Available online 8 May 2024

(Gruber et al., 2019; Witt et al., 2011), even though these findings have been challenged (Floden et al., 2015). Moreover, there is a bidirectional aspect to the association between cognition and STN DBS – *meta*-analyses comparing STN DBS and pharmacotherapy have pointed to mild, but statistically significant cognitive decline in PD patients treated with STN DBS (Combs et al., 2015; Xie et al., 2016), even though multiple randomized controlled clinical trials and observational studies reported no substantial changes in global cognitive performance (Rački et al., 2022).

The aetiology of long-term neuropsychological outcome of PD patients treated with STN DBS continues to be a matter of debate. While there have been limited reports of cognitive decline stemming from the effects of stimulation after the implantation (Reich et al., 2022; Frankemolle et al., 2010) or neuronal damage during the surgery (Witt et al., 2013; Gologorsky et al., 2011), the published cohorts are very small and proper management may generally prevent this complication. On the other hand, there is the underlying pathology of the disease itself, be it the natural course of the disease to cognitive impairment or a predisposing factor hypothesised as increased sensitivity to DBS-elicited cognitive side effects in some patients (Rački et al., 2022; Maheshwary et al., 2020). Generally, cognitive impairment in PD exhibits substantial heterogeneity in nature, severity and the risk of conversion to dementia (Cammisuli et al., 2019). Affections mostly in memory, attention and executive domains are mixed to varying degrees and often correlate with motor symptoms of PD (Pan et al., 2022; Bezdicek et al., 2018, 2019). This heterogeneity is mirrored also in imaging findings in PD-MCI. Various areas with divergent functions have been implicated, ranging from obvious candidates as prefrontal and mesiotemporal cortices, through subcortical structures and the cerebellum, up to areas not directly associated with cognitive performance as sensorimotor and occipital cortices (Jellinger, 2022). When considered in the light and complex environment of advanced therapies as STN DBS, it becomes exceedingly difficult for a clinician to differentiate between the course of the underlying neurodegeneration and adverse effects of the stimulation itself, since both may appear slowly and in DBS settings providing satisfactory relief from the primary motor symptoms (Reich et al., 2022).

However, there are currently no effective ways to predict the development of cognitive decline in STN-DBS. Test scores for attention, the age at the surgery and levodopa response have been repeatedly implicated as factors requiring attention in the selection process for STN DBS candidates (Smeding et al., 2011). Nonetheless, even in responsible adherence to these guidelines, the prevalence of cognitive impairment in STN DBS patients is non-negligible (Rački et al., 2022).

Ergo, the presented study was aimed at evaluating pre-DBS structural and microstructural cerebral patterns as possible predictors of future cognitive decline in STN DBS patients. Neuropsychological follow-up for an average of 2.3 years after STN DBS implantation procedure with consistent longitudinal use of a global cognitive test that was validated for PD-MCI diagnosis in a Czech population, the Dementia Rating Scale (DRS-2™) was the basis for a reliable differentiation between PD patients with stable cognitive performance in the post-DBS period (cognitively stable – CS) and PD patients with cognitive decline (CD). Pre-DBS cortical thickness and subcortical grey matter (GM) structure volume were utilised as proxies of structural integrity, while fractional anisotropy (FA) and mean diffusivity (MD) of both cortical and subcortical GM structures were employed to probe for microstructural characteristics as indirect markers of cellularity, myelination and cellular membrane integrity (Beaulieu, 2014). We hypothesized that PD patients who would exhibit cognitive deterioration during the post-DBS follow-up would have substantial structural and microstructural differences already prior to DBS implantation when compared to cognitively stable PD patients.

2. Methods

2.1. Subjects

In total, 90 PD patients indicated for STN DBS were enrolled into this study. They met the diagnostic criteria for clinically established PD defined by the Movement Disorders Society (Postuma et al., 2015) and the following inclusion criteria: successful bilateral STN DBS implantation within 6 months of the pre-DBS MRI acquisition and full pre-DBS DRS-2 examination, and absence of absolute exclusion criteria and red flags for PD as defined by the respective guidelines (Postuma et al., 2015). Exclusion criteria were as follows: general contraindications to MRI examination, substantial vascular or space occupying brain lesions or a neurological and/or psychiatric disorder other than PD and its related complications. The examination of cognition (DRS-2) was performed before the STN DBS implantation and then in the years 1, 3 and 5 after the surgery. The last available datapoint, i.e. with the longest follow-up duration, was utilised to calculate the DRS-2 change per year (ΔDRS-2). Subjects exhibiting DRS-2 score decline by 2 or more points per year were included into cognitive decline (CD) group; the remaining subjects were considered cognitively stable (CS). This arbitrary threshold was selected as a hypothetical rate of cognitive decline that would lead to DRS-2 score in the MCI range at the 3-year follow-up in a patient with full pre-DBS DRS-2 score of 144. Furthermore, patients who met general inclusion (diagnosis of PD, gradual cognitive decline, cognitive deficit on scale of global cognitive abilities, cognitive deficit not interfering significantly with activities of daily living) and exclusion (dementia, other primary explanations for cognitive impairment than PD, other PD-related comorbid coniditions) criteria for PD-MCI, and scored 139 or lower in DRS-2 were diagnosed with MCI at level I based on an optimal cutoff (with both specificity and sensitivity ~0.8) for PD-MCI according to the Czech normative study (Bezdicek et al., 2015; Litvan et al., 2012). MCI diagnosis was assigned to each patient independently in pre-surgery and post-surgery. And lastly, DBS-related parameters (hardware information and stimulation settings – active contacts, current/voltage-based stimulation amplitude, pulse width, stimulation frequency and therapy impedance) were recorded.

The study protocol was approved by the Ethics Committee of the General University Hospital in Prague and every subject signed a written informed consent in accordance with the Declaration of Helsinki.

2.2. Imaging protocol

The pre-DBS MRI acquisition was performed using a 3.0T MAGNETOM Skyra scanner (Siemens, Erlangen, Germany). A T1-weighted (T1w) scan was acquired with magnetisation-prepared rapid gradient echo (MPRAGE) sequence, 1.0-mm isotropic resolution, repetition time (TR) of 2,200 ms, inversion time (TI) of 900 ms, echo time (TE) of 2,43 ms and flip angle of 8°. Furthermore, the protocol included diffusion-weighted imaging (DWI), with voxel size 2.0 × 2.0 × 2.0 mm^3, TR 9,000 ms, TE 94 ms, flip angle 90°. Single b-value of 1100 s/mm^2, 30 directions with 5 additional b0 images, was acquired with antero-posterior phase encoding direction.

A follow-up post-DBS T1w scan acquired using a 1.5 T MAGNETOM Avanto scanner (Siemens, Erlangen, Germany) was utilised to evaluate the position of the DBS electrode. The following parameters were used: MPRAGE sequence with 1.0 mm isotropic resolution, TR of 2,140 ms, TI of 1,100 ms, TE of 3.93 ms and flip angle of 15°.

2.3. DBS electrode position analysis

The pipeline was based on the Lead-DBS software (Horn and Kühn, 2015) (version 2.5.3) with the enhanced workflow (Horn et al., 2019), including the optional brain shift correction (Schönecker et al., 2009). Diffeomorphic registration algorithm from Advanced Normalization Tools and subcortical refinement (Horn et al., 2019) were utilised for

spatial normalisation into the Montreal Neurological Institute (MNI). After semi-automatic electrode localisation, electric fields around the active contacts were estimated using the clinical DBS settings utilised at the time of the last available DRS-2 examination, with finite element approach and magnitude thresholding of the electric field gradient at the level of 0.2 V/mm (Vasques et al., 2009). And lastly, the overlap of the volume of tissue activated (VTA) was calculated for the following areas: the whole STN, and limbic and associative subsection of STN. The average of the left and right value were calculated to provide the mean activated volume for each of the above stated three regions of interest (ROIs).

2.4. MRI data analysis

The structural image processing pipeline included the following steps: bias-field correction, rigid-body alignment to MNI space (1-mm isotropic voxel template) and rough initial brain extraction based on non-linear (FSL FNIRT) registration of the T1w image to the MNI template, segmentation and surface reconstruction using FreeSurfer 6.0. The brain mask created by FreeSurfer was then used for the final MNI space non-linear warp. In the last step, the native-mesh surfaces of each subject were co-registered to the Conte69 average surfaces and the 2-mm standard Connectivity Informatics Technology Initiative (CIFTI) grayordinate space (Glasser et al., 2013).

DWI datasets were denoised based on random matrix theory and Marchenko-Pastur distribution (Veraart et al., 2016), utilising the optimised patch-based singular value shrinkage method (Cordero-Grande et al., 2019). Gibbs ringing artefacts were removed using the method of local subvoxel shifts (Kellner et al., 2016). These steps were followed by the correction of eddy current-induced distortions. subject movement and outlier replacement. Afterwards, DTI model was fitted to generate fractional anisotropy (FA) and mean diffusivity (MD) maps. Subcortical grey matter (GM) structures, including cerebellum were then warped to the MNI space using the matrices calculated in the T1w processing step. The cortical voxels were mapped to the subject's cortical surfaces using the partial-volume-weighted ribbon-constrained volume-to-surface mapping algorithm and resampled to the standard greyordinate space. These surface maps were then combined with the subcortical GM images to create CIFTI files.

Finally, cortical thickness maps (with regressed-out linear effects of curvature), FA and MD CIFTI files were parcellated using a combination of HCP cortical parcellation (180 parcels per hemisphere) (Glasser et al., 2016) and resting-state network-based sub-segmentation of subcortical grey matter structures with the Cole-Anticevic Brain Network Atlas (Ji et al., 2019), with size-thresholding at the level of 50 voxels per subsegment, yielding 68 subcortical ROIs. Cortical thickness maps were supplemented with volumes of subcortical structures normalised with estimated intracranial volume to create combined macrostructural CIFTI files.

2.5. Statistical analysis

Demographic and clinical data were summarised descriptively, separately for the full cohort, CS and CD subgroup. Continuous variables (age, disease duration since symptom onset, pre-DBS DRS-2, duration of follow-up, last post-DBS DRS-2, STN stimulation parameters, VTA intersection with 3 predefined STN ROIs) were compared between CS and CD subgroups using two-sample, two-tailed T-tests and categoric variables (sex, pre-DBS MCI and post-DBS MCI incidence) were compared using Fisher's exact test. Results were considered statistically significant at the predetermined alpha of 0.05 after False Discovery Rate (FDR) correction to control for multiple comparisons (Benjamini and Hochberg, 1995).

The macrostructural and microstructural correlate of pre-DBS cognitive state was analysed in a general linear model (GLM), which included pre-DBS DRS-2 total score as the predictor, and age, sex and disease duration as covariates of non-interest. The comparison of CD and CS subgroups was based on another GLM, containing CD and CS subgroup as predictors, and age, sex and disease duration as covariates of non-interest. Permutation-based non-parametric analysis as implemented in the Permutation Analysis of Linear Models package (Winkler et al., 2014) was utilised, with 10,000 permutations and FDR correction over the number of parcels separately for each modality. Results were considered significant at alpha of $p < 0.05$ and parcel cluster size thresholding of 2 to eliminate singleton cortical parcels.

3. Results

Basic demographic and clinical data, including the comparison between CS and CD in individual parameters, is provided in the Table 1. In the pre-DBS parameters, there was a statistically significant difference between CS and CD subgroups in the age at DBS implantation (average 53.65 and 63.60, respectively; $p_{FDRcor} < 0.001$) and the age of the disease onset (46 % vs 10 % of subjects in respective groups met the criteria for young-onset PD (YOPD) (Mehanna and Jankovic, 2019); $p_{FDRcor} < 0.011$). No statistically significant inter-group difference was found in the duration of the disease, pre-DBS DRS-2, presence of MCI or sex. As for the post-DBS data, only 72 out of the 90 enrolled subjects successfully underwent further DRS-2 test (14 subjects were less than 1 year after DBS implantation surgery and hadn't undergone the first neuropsychological follow-up yet at the database lock; 4 subjects had no neuropsychological follow-up). Out of these 72 PD patients, 20 (27 %) showed DRS-2 decrease of 2 or more points per year. There was no difference in the duration of follow-up between CS and CD subjects, but cognitive performance (post-DBS DRS-2, ΔDRS-2 and presence of MCI) were significantly different, where 95 % of CD patients were diagnosed with MCI at the last follow-up session (from the baseline 30 % at the pre-DBS stage). Furthermore, there was no difference in the intersection of VTA and whole STN or its subsections between the two groups. To provide better overview of the significant inter-group age difference, Fig. 1 shows the relationship between the age at DBS implantation and ΔDRS-2, distinguishing between pre-DBS MCI patients and cognitively intact PD patients.

The analysis of MRI data was based on subject numbers stated in the Table 1.

In the analysis of pre-DBS DRS-2 (90 subjects for structural data, 79 subjects for DTI data), no macrostructural, FA or MD correlate of DRS-2 was detected.

On the other hand, the comparison of the CS and CD group detected wide-spread differences both in the cerebral cortex and subcortical structures (see Fig. 2 and Table 2). CS PD patients had relatively higher cortical thickness in bilateral inferior parietal, insular and cingulate cortices, and higher volume of both putamina, but also sensorimotor and visual cortices (based on 52 CS and 20CD subjects). FA analysis (based on 46 CS and 16 CD subjects) revealed higher FA in CS PD patients in medial temporal, inferior parietal, cingulate and orbito-frontal cortex bilaterally. Subcortically, CS PD patients had relatively higher FA in the cerebellum and both hippocampi. And lastly, CS PD patients had lower MD in the inferior parietal, orbito-frontal, dorsolateral prefrontal and temporal cortices, and also in both hippocampi and the left putamen. Moreover, both MD and FA detected substantial bilateral differences between CS and CD subjects again in the occipital cortex. And lastly, due to the non-negligible differences in the average age and ratio of YOPD patients (see Table 1), two subanalyses were performed: one analysis excluding YOPD and one analysis with best possible age matching (for demographic and clinical information on these subsets, see Supplementary Tables 1 and 3). These comparisons yielded very similar regional patterns (see Supplementary Figs. 1 and 2 and Supplementary Tables 2 and 4) and effect sizes to the main analysis, albeit with lower statistical significance. Importantly, the comparison of effect sizes for the differences in the MRI modalities of interest in the clusters detected in the main analysis (see Table 2) yielded very high correlation

Table 1
Basic demographic and clinical information about the full pre-DBS cohort and available subjects in follow-up divided into stable cognitive performance and declining cognitive performance groups. Data is provided as average [standard deviation] or percentage of the full number of patients in the respective group. Abbreviations: DBS – deep brain stimulation; DRS-2 – Dementia Rating Scale; MCI – mild cognitive impairment; PD – Parkinson's disease; STN – subthalamic nucleus; AChEI – acetylcholinesterase inhibitor.

	Full cohort pre-DBS	Stable cognitive performance	Declining cognitive performance	p value FDR cor.
Number of patients	90	52	20	
With DTI available in italics	*79*	*45*	*16*	
At DBS implantation				
Age (years)	56.87 [8.78] *57.33 [8.82]*	53.65 [8.27] *54.16 [8.41]*	63.60 [5.42] *64.75 [3.55]*	**<0.001** ***<0.001***
Young-onset PD (%)	32 % *31.6 %*	46.2 % *46.7 %*	10.0 % *6.3 %*	**<0.016** ***<0.016***
Sex (% of females)	46.7 % *46.8 %*	53.8 % *51.1 %*	30.0 % *37.5 %*	0.252 *0.603*
Disease duration since symptom onset (years)	11.39 [4.58] *11.47 [4.73]*	10.94 [8.27] *11.20 [4.18]*	13.40 [5.47] *13.38 [6.12]*	0.205 *0.392*
DRS-2	139.63 [4.41] *139.48 [4.51]*	139.38 [5.06] *139.33 [5.23]*	140.45 [2.40] *139.94 [2.38]*	0.429 *0.746*
MCI (% of PD-MCI patients)	34.4 % *34.2 %*	34.6 % *35.6 %*	30.0 % *37.5 %*	0.887 *1.000*
At last neuropsychology examination				
Duration of follow-up (years)		2.35 [1.30] *2.16 [1.17]*	2.20 [1.47] *1.88 [1.45]*	0.887 *0.716*
DRS-2		140.29 [2.70] *140.42 [2.56]*	132.05 [5.54] *133.25 [4.40]*	**<0.001** ***<0.001***
MCI (% of PD-MCI patients)		26.9 % *26.7 %*	95.0 % *93.8 %*	**<0.001** ***<0.001***
DRS-2 difference per year		0.89 [3.49] *1.01 [3.70]*	−4.37 [2.11] *−4.40 [2.34]*	**<0.001** ***<0.001***
DBS-related information [number of datasets available]		51	20	
Stimulation mode [monopolar / bipolar / interleaved]		42/7/2	19/0/1	
Constant voltage / constant current mode		2/49	4/16	
Voltage amplitude (V) (bilat. average)		2.45 [0.20]	2.35 [0.65]	0.887
Current (mA) (bilat. average)		2.22 [0.70]	2.02 [0.68]	0.577
Pulse width (us)		62.25 [8.93]	63.00 [9.00]	0.887
Frequency (Hz)		127.65 [12.89]	130.00 [0.00]	0.392
Impedance (kΩ)		1192.35 [475.13]	1151.30 [391.81]	0.887
Total electrical energy delivered (μW)		52.42 [32.31]	34.61 [20.96]	0.054
Activated volume of STN (mm^3)		6.78 [11.17]	6.43 [6.09]	0.898
Associative subsection (mm^3)		2.02 [4.68]	1.81 [2.62]	0.887
Limbic subsection (mm^3)		1.13 [2.19]	0.80 [0.93]	0.603

coefficients (0.912 and 0.794 for the correlation of effect sizes in the main analysis vs subanalysis without YOPD and effect sizes in the main analysis vs age-matched-subset subanalyis, respectively; both p values < 0.001) (see Supplementary Table 5 for full information).

4. Discussion

STN DBS is a major game-changer for many PD patients, immensely improving motor symptoms and quality of life. However, it is not devoid of adverse effects, and accumulating evidence points to both the benefits and side effects stemming from specific circuits and pathways (Montgomery and Gale, 2008; Jech and Mueller, 2022). Nonetheless, this study is the first to show that patients who develop cognitive decline after DBS also differ substantially from PD DBS patients cognitively stable after DBS in both structural and microstructural brain characteristics already at the pre-DBS stage. The importance of this finding is underscored not only by the lack of differences in baseline cognitive performance, sex and disease duration between CS and CD subjects in the presented cohort, but also by the absence of significant differences in the position of DBS leads within STN and stimulation parameters (see Table 1).

The differences between CS and CD groups in MRI metrics are of an expectable nature. CS patients had relatively higher cortical thickness and subcortical GM structure volumes, which may be seen as an indication of better-preserved structural integrity or lower extent of atrophy. The microstructural findings – higher FA and lower MD – point as well to the higher presence of structures impeding free water diffusion, i.e. a higher complexity of the underlying GM tissue. Unfortunately, MRI, while a highly versatile tool sensitive to tissue alterations, remains hindered by its low specificity to the underlying histological features (Weiskopf et al., 2015). Differences in neuronal cellular density, axonal and/or dendritic structures, myelination, or even in astrocytes (Beaulieu, 2014) may be responsible for the presented results. The differences between CS and CD groups presented here are not only statistically significant, but generally provide also viable effect sizes, warranting further research. Multimodal studies combining various acquisition protocols and potentially further metrics will be necessary for relevant risk stratification and classification applicable for clinical use (Kessler et al., 2015).

The areas implicated in the CS and CD comparison (see Fig. 2 and Table 2) include regions directly related to cognition as bilateral parietal, insular and cingulate cortices, but also occipital and sensorimotor cortices, well in line with the previous reports on PD-MCI-related patterns of cortical alterations (Cammisuli et al., 2019; Jellinger, 2022). Furthermore, the microstructural DTI analysis extended the finding not only to bilateral affection of mesiotemporal and orbitofrontal cortices, but also to both hippocampi, cerebellar cortex and upper brainstem. All of these structures are vital for proper cognitive functioning in PD (Ibarretxe-Bilbao et al., 2011) and/or have been heavily implicated in the pathophysiology of PD (Simon et al., 2020). Differences detected in the cerebellum are also in line with the previous literature, given its wide range of functions in associative processes and contribution to both motor and non-motor symptoms in PD (Solstrand et al., 2020).

Importantly, the presented differences between CD and CS patients in brain macrostructure and microstructure must be considered in the light of the absence of significant inter-group differences in pre-DBS DRS-2 scores and pre-DBS incidence of MCI. Moreover, there was no correlation between cortical thickness, subcortical GM structure volume or microstructural DTI parameters with the pre-DBS DRS-2 scores, further reinforcing the putative homogeneity of the group of STN DBS candidates at the pre-DBS stage. This finding does not question the utility of DRS-2 in this setting. It merely points to the fact that the presented cohort was a carefully selected group of DBS-eligible PD patients without established major risk factors or cognitive problems, with a narrow DRS-2 distribution close to the full possible score. A wider range of DRS-2 values would probably be necessary to detect statistically

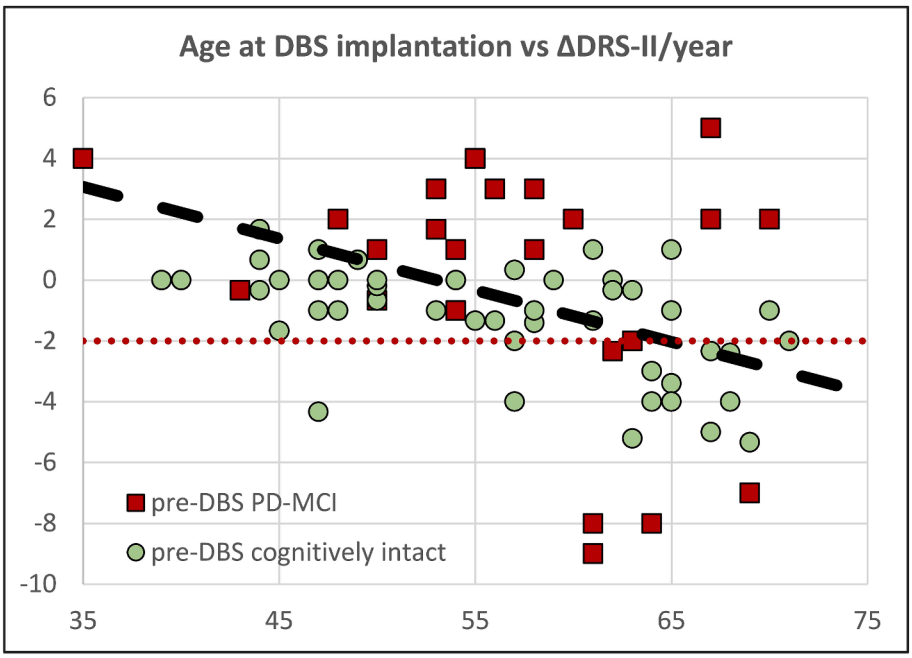

Fig. 1. Scatterplot showing the association between the within-subject DRS-2 change per year (ΔDRS-2) during the follow-up and the age at the implantation. Patients with pre-DBS mild cognitive impairment (MCI) are graphically differentiated from pre-DBS cognitively intact patients. Trendline over the full cohort is provided (black dashed line). Horizontal red dotted line represents the pre-determined ΔDRS-2 threshold for cognitive decline during the follow-up (−2 points per year). List of abbreviations: DBS – deep brain stimulation; DRS-2 – Dementia Rating Scale; PD – Parkinson's disease; MCI – mild cognitive impairment. (For interpretation of the references to colour in this figure legend, the reader is referred to the web version of this article.)

significant correlations.

Nonetheless, a major limitation must be considered when interpreting these results. Firstly, there is a substantial age difference between the CS and CD groups. While probably inherent to this subgrouping due to the higher risk of cognitive decline in higher age, the well-known dependence of all the implemented MRI metrics on age is a factor difficult to account for, despite the inclusion of age and disease duration as nuisance covariates in the GLMs. True, multiple areas of high relevance for the cognitive performance are exceedingly susceptible to alterations seen in ageing, but the patterns implicated in this study do not correspond fully to the repeatedly published antero-posterior gradient of age-related changes with dominant affection of prefrontal cortices (Boban et al., 2022; Karolis et al., 2019). Furthermore, the age ranges included in this study are generally still in the area of gentler slopes before the often quadratic, steep changes seen in multiple MRI metrics in higher age groups (Filip et al., 2023). Nonetheless, the interaction of ageing and neurodegenerative processes is a matter of exceeding complexity, and while there are preliminary indications pointing to increased ageing rate in neurodegenerative diseases (Beheshti et al., 2020; Eickhoff et al., 2021), multimodal longitudinal studies will be of essence to shed light on this issue. But most importantly for the presented study, supplementary sub-analyses in a subset excluding YOPD subjects and a subset limited to age-matched subgroups yielded very similar regional distribution and effect sizes of detected differences to the main analysis, indicating that the presented findings are, to a major part, interpretable as age-independent. Due to the relative scarcity of suitable subjects, further studies should encompass multi-site endeavours to collect datasets of sufficient size where more detailed hypotheses related to cognitive decline in STN DBS could be evaluated Secondly, the only outcome measure of cognitive function in the presented study was DRS-2. Although previously validated for use in PD patients in a Czech population and appropriately suitable for cognitive screening of global cognition, DRS-2 does not appear to have utility in evaluating single cognitive functions in PD (Lopez et al., 2023; Boel et al., 2022). Further studies using more complex assessment of cognition (e.g. level II diagnosis of PD-MCI) will be necessary to evaluate whether our results correspond to the type of cognitive deficit which may develop after DBS implantation.

5. Conclusion

All in all, this is the first study showing substantial pre-implantation cortical and subcortical differences between PD patients who would exhibit post-DBS cognitive decline and PD patients with stable cognitive performance during the post-DBS follow-up. Moreover, cognitive decline in the presented cohort was not directly attributable to the position of DBS leads within STN or utilised stimulation parameters – i.e. not attributable to STN DBS primarily, but to this clinically silent structural and microstructural predisposition to future cognitive deterioration present already before STN DBS implantation.

Funding statement

Support was provided by the Czech Ministry of Health (AZV NV19-04-00233) and the General University Hospital in Prague (MH CZ-DRO-VFN64165) and Na Homolce Hospital (MH CZ-DRO-NNH 23884). In addition, this project has received funding from the European Union's Horizon 2020 research and innovation programme under the JPND2020-568-028 – Neuripides, National Institute for Neurological Research, Czech Republic, Programme EXCELES (ID project No. LX22NPO5107), Grant Agency of Charles University under the GA UK 254121 and Charles University, Czech Republic – Cooperatio Program in Neuroscience.

Code availability

Not applicable.

Authors' contributions

P.F. designed the data analysis approach, performed the MRI and clinical data analysis, created the figures and tables and wrote the

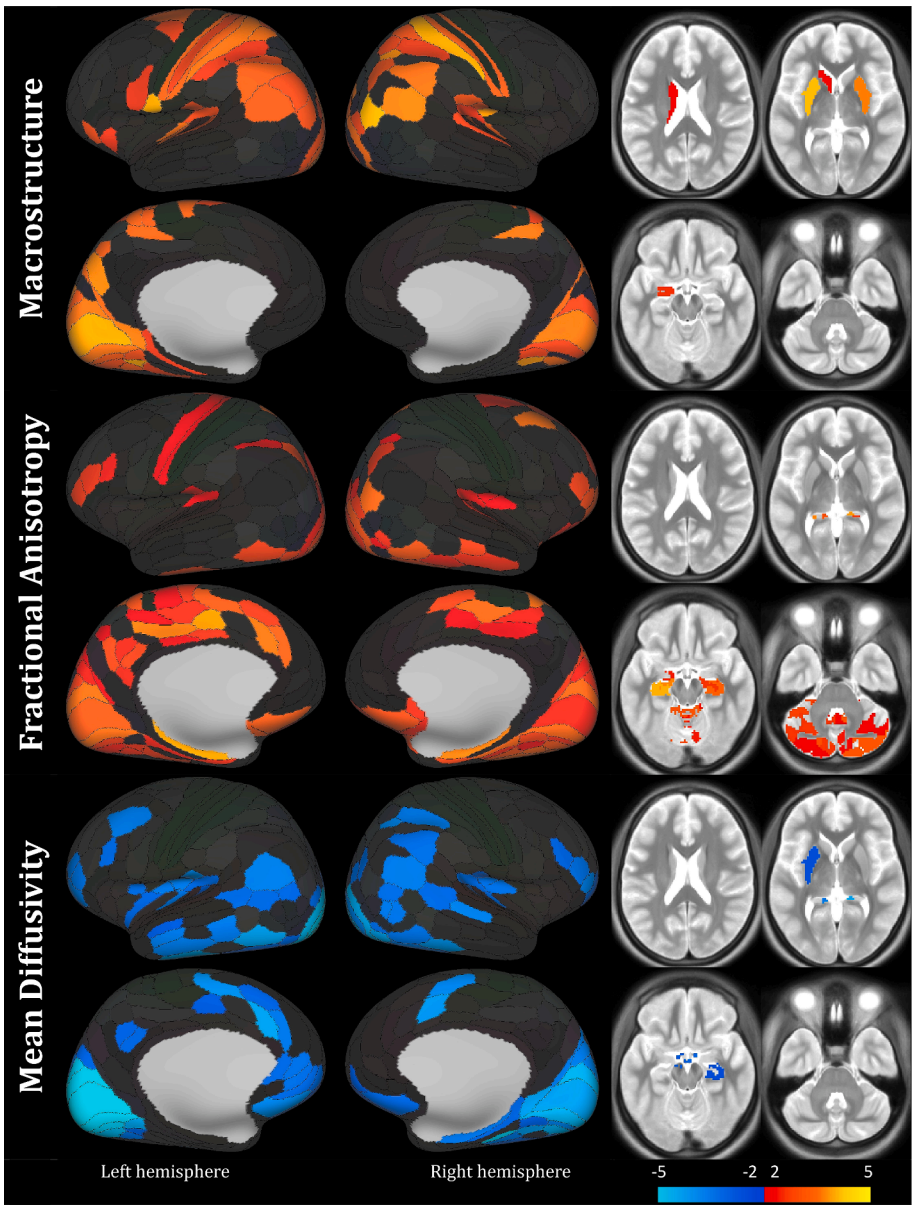

Fig. 2. Main results for the comparison of patients with stable cognitive performance (CS) and declining cognitive performance (CD) for parcellated structural data (cerebral cortical thickness + subcortical grey matter structure volume), fractional anisotropy and mean diffusivity. Alpha of 0.05, false discovery rate corrected. Red-yellow scale marks CS > CD contrast, blue scale labels the reverse contrast; values correspond to the T statistic. Subcortical structures shown in 4 slices z = 20, 2, −16, −34 (MNI coordinate system). Laterality convention where the right side of the figure corresponds to the right side of the brain is used. See Table 2 for further anatomical and statistical information on significant regions. Abbreviations: L – left; R – right. For the full list of abbreviations and information on individual parcels utilised as nodes, see (Glasser et al., 2016). (For interpretation of the references to colour in this figure legend, the reader is referred to the web version of this article.)

manuscript. J.M. performed the evaluation of cognition and edited the manuscript. A.L. performed the Lead-DBS analysis, curated the database and edited the manuscript. J.K. managed the data acquisition and edited the manuscript. D.U. and J.May participated in data acquisition and edited the manuscript. K.M. edited the manuscript. F.R., R.J., O.B. designed the primary hypothesis, secured funding for the project and edited the manuscript.

Ethics approval

The study protocol was approved by the ethics committee of the General University Hospital in Prague, Czech Republic.

Consent to participate

Each subject provided a written informed consent in accordance with the Declaration of Helsinki.

CRediT authorship contribution statement

Pavel Filip: Writing – original draft, Visualization, Software, Project administration, Methodology, Formal analysis, Data curation, Conceptualization. **Josef Mana:** Writing – review & editing, Investigation, Data curation, Conceptualization. **Andrej Lasica:** Writing – review & editing, Formal analysis, Data curation. **Jiří Keller:** Writing – review & editing, Data curation. **Dušan Urgošík:** Writing – review & editing, Data curation. **Jaromír May:** Writing – review & editing, Data curation. **Karsten Mueller:** Writing – review & editing. **Robert Jech:** Writing – review &

Table 2
Results of parcellated comparison of patients with stable cognitive performance (CS) and declining cognitive performance (CD) for structural data (cerebral cortical thickness + subcortical grey matter structure volume normalised by estimated intracranial volume), fractional anisotropy and mean diffusivity [mean diffusivity values multiplied by the factor of 1,000 for better legibility]. Data reported as clusters, with cortical anatomical localisation based on 22 main cortical segments and parcellation as defined by (Glasser et al., 2016), number of parcellation regions of interest contained in each cluster (column #), average and standard deviation separately for CS and CD group, effect size (Cohen's d), T statistic of permutation-based T test and p value. Alpha of 0.05, False Discovery Rate corrected was implemented. Individual entries are sorted in descending order based on the effect size. See also Fig. 2. Abbreviations: T stat – T statistic; Macrostructure – macrostructural data (cortical thickness and subcortical grey matter structure volumes); FDR – False Discovery Rate; L – left; R – right.

	Side and anatomical area		#	Stableperformance	Declining performance	Effect size	T stat	p val (FDR)
Macrostructure [mm for cortex, unitless for subcort. areas]	L	Dorsal Stream Visual, Early Visual, Posterior Cingulate, Ventral Stream Visual, Medial Temporal, Primary Visual, Superior Parietal and IPS	16	2.237 [0.127]	2.043 [0.149]	1.402	3.933	0.008
	R	Superior Parietal and IPS, Inferior Parietal, Dorsal Stream Visual, Somatosensory and Motor, Early Visual, Paracentral Lobular and Mid Cingulate, Ventral Stream Visual, MT + Complex and neighbouring Visual Areas, Posterior Cingulate, Primary Visual	24	2.191 [0.160]	1.996 [0.144]	1.280	4.080	0.008
	R	Posterior Operculum, Early Auditory, Auditory Association, Insular	7	2.557 [0.198]	2.353 [0.122]	1.243	3.788	0.011
	L	Putamen	2	0.302 [0.035]	0.265 [0.028]	1.151	4.174	0.008
	L	Inferior Parietal, Somatosensory and Motor, Paracentral Lobular and Mid Cingulate, Superior Parietal and IPS, Posterior Operculum, Premotor	18	2.223 [0.149]	2.064 [0.140]	1.105	3.981	0.011
	L	Early Auditory, Insular, Posterior Operculum	5	2.480 [0.191]	2.274 [0.207]	1.033	3.290	0.018
	R	Putamen	1	0.303 [0.037]	0.270 [0.029]	1.020	3.686	0.008
	L	Paracentral Lobular and Mid Cingulate, Premotor	4	2.525 [0.196]	2.350 [0.234]	0.812	3.003	0.023
	L	Inferior Frontal, Insular	2	2.774 [0.229]	2.598 [0.212]	0.795	2.597	0.033
	L	Amygdala	4	0.103 [0.014]	0.094 [0.015]	0.673	2.595	0.036
	L	Caudate	2	0.218 [0.029]	0.202 [0.018]	0.665	2.305	0.050
Fractional Anisotropy [unitless]	R	Hippocampus	3	0.174 [0.033]	0.133 [0.024]	1.405	3.880	0.010
	L	Hippocampus	3	0.158 [0.024]	0.129 [0.022]	1.223	4.066	0.010
	R	Ventral Stream Visual, Medial Temporal, Dorsal Stream Visual, MT + Complex and neighbouring Visual Areas, Early Visual, Lateral Temporal, Inferior Parietal, Posterior Cingulate, Primary Visual, Superior Parietal and IPS	30	0.128 [0.017]	0.109 [0.017]	1.092	3.589	0.010
	L	Dorsal Stream Visual, Medial Temporal, Early Visual, Ventral Stream Visual, Lateral Temporal, MT + Complex and Neighboring Visual Areas, Posterior Cingulate, Primary Visual	19	0.127 [0.019]	0.109 [0.021]	0.886	3.947	0.010
	L	Amygdala	1	0.154 [0.047]	0.123 [0.021]	0.849	2.452	0.010
	R	Paracentral Lobular and Mid Cingulate, Posterior Cingulate, Superior Parietal and IPS	7	0.114 [0.015]	0.099 [0.020]	0.815	3.273	0.015
	R	Cerebellum	4	0.167 [0.017]	0.154 [0.015]	0.807	3.163	0.010
	L	Inferior Frontal	3	0.130 [0.024]	0.113 [0.018]	0.806	2.387	0.030
	L	Orbital and Polar Frontal	3	0.186 [0.054]	0.149 [0.044]	0.756	2.827	0.020
	L	Cerebellum	4	0.176 [0.020]	0.159 [0.026]	0.748	3.031	0.017
	R	Orbital and Polar Frontal, Inferior Frontal, Anterior Cingulate, Insular	11	0.161 [0.032]	0.140 [0.027]	0.730	2.645	0.016
	R	Early Auditory, Insular, Posterior Operculum	5	0.132 [0.033]	0.118 [0.021]	0.506	2.129	0.027
	L	Early Auditory, Posterior Operculum	2	0.135 [0.041]	0.120 [0.018]	0.466	1.982	0.033
	L	Paracentral Lobular and Mid Cingulate, Anterior Cingulate, Posterior Cingulate, Somatosensory and Motor, Superior Parietal and IPS	15	0.125 [0.013]	0.115 [0.028]	0.425	3.792	0.010
	R	Dorsolateral Prefrontal, Premotor	4	0.121 [0.016]	0.114 [0.020]	0.412	3.278	0.010
	L	Posterior Cingulate, Superior Parietal and IPS	5	0.118 [0.018]	0.112 [0.024]	0.306	2.584	0.016
	L	Inferior Parietal	2	0.126 [0.027]	0.116 [0.046]	0.256	2.525	0.021
Mean diffusivity [1,000 × mm^2/s]	L	Ventral Stream Visual, Lateral Temporal, Early Visual, Dorsal Stream Visual, MT + Complex and neighbouring Visual Areas, Auditory Association, Primary Visual	18	0.966 [0.060]	1.062 [0.057]	1.631	−5.539	0.007
	R	Ventral Stream Visual, Medial Temporal, Early Visual, Dorsal Stream Visual, MT + Complex and neighbouring Visual Areas, Posterior Cingulate, Inferior Parietal, Lateral Temporal, Primary Visual	22	1.004 [0.066]	1.116 [0.075]	1.595	−4.883	0.007
	L	Anterior Cingulate, Orbital and Polar Frontal, Paracentral Lobular and Mid Cingulate, Dorsolateral Prefrontal, Inferior Frontal	16	0.907 [0.055]	0.999 [0.069]	1.472	−3.942	0.009
	R	Superior Parietal and IPS	2	1.056 [0.095]	1.180 [0.077]	1.431	−3.328	0.016
	R	Anterior Cingulate, Paracentral Lobular and Mid Cingulate	2	0.905 [0.058]	0.982 [0.073]	1.161	−3.703	0.009
	R	Orbital and Polar Frontal, Inferior Frontal	8	0.902 [0.086]	0.992 [0.071]	1.143	−3.216	0.024
	L	Insular, Early Auditory, Posterior Operculum	8	0.944 [0.056]	1.019 [0.078]	1.098	−3.336	0.014
	R	Early Auditory, Insular, Posterior Operculum	6	0.963 [0.068]	1.036 [0.066]	1.083	−2.896	0.025
	R	Hippocampus	2	1.018 [0.204]	1.291 [0.303]	1.056	−4.344	0.007
	L	Hippocampus	1	1.057 [0.240]	1.294 [0.207]	1.055	−3.510	0.014
	R	Inferior Parietal, MT + Complex and neighbouring Visual Areas, Temporal-Parietal-Occipital Junction, Auditory Association	7	0.938 [0.063]	1.014 [0.083]	1.030	−3.239	0.024

(*continued on next page*)

Table 2 (*continued*)

	Side and anatomical area	#	Stableperformance	Declining performance	Effect size	T stat	p val (FDR)
L	Temporal-Parietal-Occipital Junction, Inferior Parietal	4	0.931 [0.064]	1.009 [0.088]	1.010	−3.161	0.016
R	Diencephalon ventral	1	0.981 [0.161]	1.120 [0.142]	0.911	−3.048	0.025
L	Dorsolateral Prefrontal, Inferior Frontal	2	0.920 [0.082]	1.018 [0.145]	0.831	−3.127	0.025
L	Posterior Cingulate	2	0.933 [0.066]	0.987 [0.065]	0.817	−2.648	0.037
L	Diencephalon ventral	1	0.914 [0.105]	1.000 [0.112]	0.795	−2.781	0.034
L	Putamen	1	0.750 [0.028]	0.774 [0.041]	0.678	−2.592	0.037

editing, Validation, Supervision, Funding acquisition, Conceptualization. **Ondrej Bezdicek:** Writing – review & editing, Funding acquisition. **Filip Růžička:** Writing – review & editing, Funding acquisition.

Declaration of competing interest

The authors declare that they have no known competing financial interests or personal relationships that could have appeared to influence the work reported in this paper.

Data availability

The MRI datasets of the presented study are not publicly available due to the sensitive nature and data privacy regulations related to patient data. However, they are available from the corresponding author upon reasonable request.

Appendix A. Supplementary data

Supplementary data to this article can be found online at https://doi.org/10.1016/j.nicl.2024.103617.

References

Beaulieu, C., 2014. The biological basis of diffusion anisotropy. In: Diffusion MRI. Elsevier, pp. 155–183.

Beheshti, I., Mishra, S., Sone, D., Khanna, P., Matsuda, H., 2020. T1-Weighted MRI-Driven brain age estimation in Alzheimer's disease and Parkinson's disease. Aging Dis. 11 (3), 618–628. https://doi.org/10.14336/AD.2019.0617.

Benjamini, Y., Hochberg, Y., 1995. Controlling the false discovery rate: a practical and powerful approach to multiple testing. J. Roy. Stat. Soc.: Ser. B (Methodol.) 57 (1), 289–300.

Bezdicek, O., Michalec, J., Nikolai, T., Havránková, P., Roth, J., Jech, R., R\uužička, E., 2015. Clinical validity of the Mattis dementia rating scale in differentiating mild cognitive impairment in Parkinson's disease and normative data. Dement. Geriatr. Cogn. Disord. 39 (5–6), 303–311.

Bezdicek, O., Ballarini, T., R\uužička, F., Roth, J., Mueller, K., Jech, R., Schroeter, M.L., 2018. Mild cognitive impairment disrupts attention network connectivity in Parkinson's disease: combined multimodal MRI and meta-analytical study. Neuropsychologia 112, 105–115.

Bezdicek, O., Ballarini, T., Buschke, H., Růžička, F., Roth, J., Albrecht, F., Růžička, E., Mueller, K., Schroeter, M.L., Jech, R., 2019. Memory impairment in Parkinson's disease: the retrieval versus associative deficit hypothesis revisited and reconciled. Neuropsychology 33 (3), 391–405. https://doi.org/10.1037/neu0000503.

Boban, Jasmina, Thurnher, M.M., Boban, N., Law, M., Jahanshad, N., Nir, T.M., Lendak, D.F., Kozic, D., 2022. Gradient patterns of age-related diffusivity changes in cerebral white matter. Front. Neurol. 13. doi:10.3389/fneur.2022.870909.

Boel, J.A., de Bie, R.M.A., Schmand, B.A., Dalrymple-Alford, J.C., Marras, C., Adler, C.H., Goldman, J.G., et al., 2022. Level I PD-MCI using global cognitive tests and the risk for Parkinson's disease dementia. Movement Disorders Clinical Practice 9 (4), 479–483. https://doi.org/10.1002/mdc3.13451.

Cammisuli, D.M., Cammisuli, S.M., Fusi, J., Franzoni, F., Pruneti, C., 2019. Parkinson's disease–mild cognitive impairment (PD-MCI): A useful summary of update knowledge. Front. Aging Neurosci. 11, 303.

Combs, H.L., Folley, B.S., Berry, D.TR., Segerstrom, S.C., Han, D.Y., Anderson-Mooney, A.J., Walls, B.D., van Horne, C., 2015. Cognition and depression following deep brain stimulation of the subthalamic nucleus and globus pallidus pars internus in Parkinson's disease: a meta-analysis. Neuropsychol. Rev. 25, 439–454.

Cordero-Grande, L., Christiaens, D., Hutter, J., Price, A.N., Hajnal, J.V., 2019. Complex diffusion-weighted image estimation via matrix recovery under general noise models. Neuroimage 200 (říjen), 391–404. https://doi.org/10.1016/j.neuroimage.2019.06.039.

Eickhoff, C.R., Hoffstaedter, F., Caspers, J., Reetz, K., Mathys, C., Dogan, I., Amunts, K., Schnitzler, A., Eickhoff, S.B., 2021. Advanced brain ageing in Parkinson's disease is related to disease duration and individual impairment. Brain Commun. 3(3), fcab191. https://doi.org/10.1093/braincomms/fcab191.

Filip, P., Kokošová, V., Valenta, Z., Baláž, M., Mangia, S., Michaeli, S., Vojtíšek, L., 2023. Utility of quantitative MRI metrics in brain ageing research. Front. Aging Neurosci. 15.

Floden, D., Busch, R.M., Cooper, S.E., Kubu, C.S., Machado, A.G., 2015. Global cognitive scores do not predict outcome after subthalamic nucleus deep brain stimulation. Movement Disorders 30 (9), 1279–1283. https://doi.org/10.1002/mds.26292.

Frankemolle, A.MM., Jennifer, Wu., Noecker, A.M., Voelcker-Rehage, C., Ho, J.C., Vitek, J.L., McIntyre, C.C., Alberts, J.L., 2010. Reversing cognitive–motor impairments in Parkinson's disease patients using a computational modelling approach to deep brain stimulation programming. Brain 133 (3), 746–761.

Glasser, M.F., Sotiropoulos, S.N., Anthony Wilson, J., Coalson, T.S., Fischl, B., Andersson, J.L., Junqian, Xu., Jbabdi, S.a., Webster, M., Polimeni, J.R., 2013. The minimal preprocessing pipelines for the Human Connectome Project. Neuroimage 80, 105–124.

Glasser, M.F., Coalson, T.S., Robinson, E.C., Hacker, C.D., Harwell, J., Yacoub, E., Ugurbil, K., Andersson, J., Beckmann, C.F., Jenkinson, M., 2016. A multi-modal parcellation of human cerebral cortex. Nature 536 (7615), 171–178.

Gologorsky, Y., Ben-Haim, S., Moshier, E.L., Godbold, J., Tagliati, M., Weisz, D., Alterman, R.L., 2011. Transgressing the ventricular wall during subthalamic deep brain stimulation surgery for Parkinson disease increases the risk of adverse neurological sequelae. Neurosurgery 69 (2), 294–300.

Gruber, D., Calmbach, L., Kühn, A.A., Krause, P., Kopp, U.A., Schneider, G.-H., Kupsch, A., 2019. Longterm outcome of cognition, affective state, and quality of life following subthalamic deep brain stimulation in Parkinson's disease. J. Neural Transm. 126 (3), 309–318. https://doi.org/10.1007/s00702-019-01972-7.

Horn, A., Kühn, A.A., 2015. Lead-DBS: a toolbox for deep brain stimulation electrode localizations and visualizations. Neuroimage 107, 127–135.

Horn, A., Li, N., Dembek, T.A., Kappel, A., Boulay, C., Ewert, S., Tietze, A., Husch, A., Perera, T., Neumann, W.-J., 2019. Lead-DBS v2: towards a comprehensive pipeline for deep brain stimulation imaging. Neuroimage 184, 293–316.

Ibarretxe-Bilbao, N., Junque, C., Marti, M.J., Tolosa, E., 2011. Brain structural MRI correlates of cognitive dysfunctions in Parkinson's disease. J. Neurol. Sci. 310 (1), 70–74. https://doi.org/10.1016/j.jns.2011.07.054.

Jech, R., Mueller, K., 2022. Investigating network effects of DBS with fMRI. In: Connectomic Deep Brain Stimulation. Elsevier, pp. 275–301.

Jellinger, K.A., 2022. Morphological basis of Parkinson disease-associated cognitive impairment: an update. J. Neural Transm. 129 (8), 977–999.

Ji, J.L., Spronk, M., Kulkarni, K., Repovš, G., Anticevic, A., Cole, M.W., 2019. Mapping the human Brain's cortical-subcortical functional network organization. Neuroimage 185, 35–57. https://doi.org/10.1016/j.neuroimage.2018.10.006.

Jr, M., Erwin, B., Gale, J.T., 2008. Mechanisms of action of deep brain stimulation (DBS). Neurosci. Biobehav. Rev. 32 (3), 388–407.

Karolis, V.R., Callaghan, M.F., Tseng, C.-E., Hope, T., Weiskopf, N., Rees, G., Cappelletti, M., 2019. Spatial gradients of healthy aging: a study of myelin-sensitive maps. Neurobiol. Aging 79 (červenec), 83–92. https://doi.org/10.1016/j.neurobiolaging.2019.03.002.

Kellner, E., Dhital, B., Kiselev, V.G., Reisert, M., 2016. Gibbs-ringing artifact removal based on local subvoxel-shifts. Magn. Reson. Med. 76 (5), 1574–1581.

Kessler, L.G., Barnhart, H.X., Buckler, A.J., Choudhury, K.R., Kondratovich, M.V., Toledano, A., Guimaraes, A.R., Filice, R., Zhang, Z., Sullivan, D.C., 2015. The emerging science of quantitative imaging biomarkers terminology and definitions for scientific studies and regulatory submissions. Stat. Methods Med. Res. 24 (1), 9–26.

Litvan, I., Goldman, J.G., Tröster, A.I., Schmand, B.A., Weintraub, D., Petersen, R.C., Mollenhauer, B., et al., 2012. Diagnostic criteria for mild cognitive impairment in Parkinson's disease: *movement* disorder society task force guidelines. Mov. Disord. 27 (3), 349–356. https://doi.org/10.1002/mds.24893.

Lopez, F.V., Kenney, L.E., Ratajska, A., Jacobson, C.E., Bowers, D., 2023. What does the dementia rating scale-2 measure? The relationship of neuropsychological measures to DRS-2 total and subscale scores in non-demented individuals with Parkinson's disease. Clin. Neuropsychol. 37 (1), 174–193. https://doi.org/10.1080/13854046.2021.1999505.

Maheshwary, A., Mohite, D., Omole, J.A., Bhatti, K.S., Khan, S., 2020. Is deep brain stimulation associated with detrimental effects on cognitive functions in patients of Parkinson's disease? A systematic review. Cureus 12 (8).

Mehanna, R., Jankovic, J., 2019. Young-onset Parkinson's disease: Its unique features and their impact on quality of life. Parkinsonism Relat. Disord. 65 (srpen), 39–48. https://doi.org/10.1016/j.parkreldis.2019.06.001.

Pan, C., Li, Y., Ren, J., Li, L., Huang, P., Pingyi, Xu., Zhang, L.i., et al., 2022. Characterizing mild cognitive impairment in prodromal Parkinson's disease: a community-based study in China. CNS Neurosci. Ther. 28 (2), 259–268. https://doi.org/10.1111/cns.13766.

Postuma, R.B., Berg, D., Stern, M., Werner Poewe, C., Olanow, W., Oertel, W., Obeso, J., Marek, K., Litvan, I., Lang, A.E., 2015. MDS clinical diagnostic criteria for Parkinson's disease". Mov. Disord. 30 (12), 1591–1601.
Rački, V., Hero, M., Rožmarić, G., Papić, E., Raguž, M., Chudy, D., Vuletić, V., 2022. Cognitive impact of deep brain stimulation in Parkinson's disease patients: a systematic review. Front. Hum. Neurosci. 16, 867055.
Reich, M.M., Hsu, J., Ferguson, M., Schaper, F.L., Joutsa, J., Roothans, J., Nickl, R.C., Frankemolle-Gilbert, A., Alberts, J., Volkmann, J., 2022. A brain network for deep brain stimulation induced cognitive decline in Parkinson's disease. Brain 145 (4), 1410–1421.
Schönecker, T., Kupsch, A., Kühn, A.A., Schneider, G.-H., Hoffmann, K.-T., 2009. Automated optimization of subcortical cerebral MR imaging- atlas coregistration for improved postoperative electrode localization in deep brain stimulation. Am. J. Neuroradiol. 30 (10), 1914–1921.
Simon, D.K., Tanner, C.M., Brundin, P., 2020. Parkinson disease epidemiology, pathology, genetics, and pathophysiology. Clin. Geriatr. Med. 36 (1), 1–12.
Smeding, H.MM., Speelman, J.D., Huizenga, H.M., Richard Schuurman, P., Schmand, B., 2011. Predictors of cognitive and psychosocial outcome after STN DBS in Parkinson's disease. J. Neurol. Neurosurg. Psychiatry 82 (7), 754–760.
Solstrand, L.D., Linda, O.L., Doyon, J., 2020. Cerebellar contribution to motor and non-motor functions in Parkinson's disease: a meta-analysis of fMRI findings. Front. Neurol. 11. https://doi.org/10.3389/fneur.2020.00127.
Vasques, X., Cif, L., Hess, O., Gavarini, S., Mennessier, G., Coubes, P., 2009. Stereotactic model of the electrical distribution within the internal globus pallidus during deep brain stimulation. J. Comput. Neurosci. 26 (1), 109.
Veraart, J., Fieremans, E., Novikov, D.S., 2016. Diffusion MRI noise mapping using random matrix theory. Magn. Reson. Med. 76 (5), 1582–1593.
Weiskopf, N., Mohammadi, S., Lutti, A., Callaghan, M.F., 2015. Advances in MRI-based computational neuroanatomy: from morphometry to in-vivo histology. Curr. Opin. Neurol. 28 (4), 313–322.
Winkler, A.M., Ridgway, G.R., Webster, M.A., Smith, S.M., Nichols, T.E., 2014. Permutation inference for the general linear model. Neuroimage 92 (kvèten), 381–397. https://doi.org/10.1016/j.neuroimage.2014.01.060.
Witt, K., Daniels, C., Krack, P., Volkmann, J., Pinsker, M.O., Kloss, M., Tronnier, V., et al., 2011. Negative impact of borderline global cognitive scores on quality of life after subthalamic nucleus stimulation in Parkinson's disease. J. Neurol. Sci. 310 (1–2), 261–266. https://doi.org/10.1016/j.jns.2011.06.028.
Witt, K., Granert, O., Daniels, C., Volkmann, J., Falk, D., van Eimeren, T., Deuschl, G., 2013. Relation of lead trajectory and electrode position to neuropsychological outcomes of subthalamic neurostimulation in Parkinson's disease: results from a randomized trial. Brain 136 (7), 2109–2119.
Xie, Y., Meng, X., Xiao, J., Zhang, J., Zhang, J., 2016. Cognitive changes following bilateral deep brain stimulation of subthalamic nucleus in Parkinson's disease: a meta-analysis. BioMed Res. Int..